Source Bearing and Steering-Vector Estimation using Partially Calibrated Arrays

MINGHUI LI, Member, IEEE
University of Strathclyde

YILONG LU, Member, IEEE
Nanyang Technological University

The problem of source direction-of-arrival (DOA) estimation using a sensor array is addressed, where some of the sensors are perfectly calibrated, while others are uncalibrated. An algorithm is proposed for estimating the source directions in addition to the estimation of unknown array parameters such as sensor gains and phases, as a way of performing array self-calibration. The cost function is an extension of the maximum likelihood (ML) criteria that were originally developed for DOA estimation with a perfectly calibrated array. A particle swarm optimization (PSO) algorithm is used to explore the high-dimensional problem space and find the global minimum of the cost function. The design of the PSO is a combination of the problem-independent kernel and some newly introduced problem-specific features such as search space mapping, particle velocity control, and particle position clipping. This architecture plus properly selected parameters make the PSO highly flexible and reusable, while being sufficiently specific and effective in the current application. Simulation results demonstrate that the proposed technique may produce more accurate estimates of the source bearings and unknown array parameters in a cheaper way as compared with other popular methods, with the root-mean-squared error (RMSE) approaching and asymptotically attaining the Cramer Rao bound (CRB) even in unfavorable conditions.

Manuscript received February 1, 2007; revised March 23 and July 28, 2008; released for publication August 4, 2008.

IEEE Log No. T-AES/45/4/935098.

Refereeing of this contribution was handled by P. Lombardo.

Authors' addresses: M. Li, Dept. of Electronic and Electrical Engineering, University of Strathclyde, Royal College Bldg., 204 George St., Glasgow G1 1XW, UK, E-mail: (Minghui.Li@ieee.org); Y. Lu, School of Electrical and Electronic Engineering, Nanyang Technological University, Nanyang Ave., Singapore 639798.

0018-9251/09/$26.00 © 2009 IEEE

I. INTRODUCTION

Source direction-of-arrival (DOA) estimation using a partially calibrated array (PCA) with a mixture of two types of sensors (calibrated and uncalibrated) is an important, but challenging problem, which arises in many practical applications. For example, we want to augment a well-constructed array by placing a number of additional sensors to enlarge the aperture. Since these elements are placed in the field, there is no opportunity to calibrate them. Another example is in the situation where one or more array elements are damaged. Although the defective elements can be rectified by replacement, calibration of these elements may be a much more complicated task and the process might be too time-consuming, especially for arrays performing critical operations. In these cases, the response of the additional or replaced elements may be poorly known or completely unknown due to amplitude and phase mismatch of the receivers, inaccurate sensor location, and imperfect sensor gain or phase characteristics, or a combination of these effects, while the other elements are well calibrated. Weiss and Friedlander [1] confirm that the direction finding performance of a calibrated array can be enhanced by the addition of completely uncalibrated elements.

Since almost all high-resolution direction-finding techniques such as multiple signal classification (MUSIC), estimation of signal parameters via rotational invariance techniques (ESPRIT), weighted subspace fitting (WSF), as well as maximum likelihood (ML) algorithms [2–5], are sensitive even to small array manifold model errors and require perfect array calibration, direct application of these techniques to PCAs for DOA estimation seems unrealistic [6]. For completely uncalibrated arrays, estimation of the steering vectors and signal parameters is only possible for non-Gaussian signals by using high-order statistics of the received data [7]. The problem is sometimes referred to as the blind estimation problem. However, by introducing some additional constraints into the problem, estimation based on second-order moments is possible. The previous works can be classified into three categories according to the problem formulation. Some researchers attempt to estimate the signal DOAs without jointly exploiting the knowledge of the unknown manifold parameters using particular array structures. The rank reduction estimators (RARE) [8] are developed for partly calibrated sparse arrays composed of multiple subarrays with the underlying assumption that the manifold of each subarray is known exactly but there is no calibration between subarrays. The method of [9] is based on the assumption that the calibrated sensors and the uncalibrated sensors are well separated.

Authorized licensed use limited to: STRATHCLYDE UNIVERSITY LIBRARY. Downloaded on July 01,2010 at 09:09:56 UTC from IEEE Xplore. Restrictions apply.

The methods in the second category are derived for estimating the sensor gain and phase characteristics when certain source parameters are known exactly. In [10], an algorithm is presented based on the assumption that the covariance matrix of the field variables at the sensor locations is known. In [11], [12] the problems are addressed assuming that the source DOAs are known. Another main approach is to jointly estimate the source DOAs and unknown array parameters with certain constrains. The method of [13] treats the case of steering vectors with known gain and unknown phases and uncorrelated sources. The same model with correlated sources is discussed in [14]. In [15]–[17], algorithms are derived under the assumption that the uncalibrated sensors have unknown angularly independent gains and arbitrary phases, where the sources are uncorrelated.

In this paper, we develop an algorithm based on the ML methodology for joint estimation of source DOAs and gains and phases of uncalibrated sensors in a PCA. The cost function is an extension of the ML criteria that were originally developed for angle estimation with a perfectly calibrated array. As in [16], [17], the uncalibrated array elements are assumed to have unknown angularly independent gains, and arbitrary and unknown phases. However, the sources can be correlated, even coherent.

In most of the published works, the estimates of unknown parameters are computed by optimizing a nonlinear complicated cost function, and Newton-type techniques are preferred to global search methods as the computing tools. The main reason is that conventional global optimization algorithms are prone to suffering from slow convergence and require huge computation [18]. One of the most popular global search techniques is genetic algorithms (GA), which are stochastic search algorithms based on the mechanism of natural selection where fitter individuals have higher chances to survive in a competing environment; however, it is also known as a slow optimization tool [19]. On the other hand, Newton-type methods intrinsically are local search techniques, where global convergence cannot be guaranteed and sufficiently good initialization is crucial for a success. Furthermore, a Newton-type method is not always a guarantee of efficiency in computation.

Instead of using a Newton-type procedure, we present a more reliable and robust global search algorithm—particle swarm optimization (PSO) algorithm for finding the minimum of the cost function. PSO is a recent addition to evolutionary algorithms first introduced by Eberhart and Kennedy in 1995 [20]. The foundation of PSO is based on the hypothesis that social sharing of information among conspecifics offers an evolutionary advantage. Partially inspired by animal social behaviors such as flocking of birds, PSO originally intends to graphically mimic the graceful way in which they find their food sources and save themselves from predators. PSO is a population-based stochastic optimization paradigm, in which each agent, named particle, of the population, named swarm, is thought of as a collision-proof bird and used to represent a potential solution. As an emerging technology, PSO has attracted a lot of attention in recent years, and has been successfully applied in many fields, such as direction finding in spatially correlated noise [21], phased array synthesis [22], electromagnetic optimization [23], blind source separation [24], artificial neural network training [25], power flow optimization [26], task assignment [27], and etc. Most of the applications demonstrated that PSO could give competitive or even better results in a faster and cheaper way, compared with other heuristic methods such as GA. In addition, PSO appears to be robust to control parameters.

Due to the multimodal, nonlinear and high-dimensional nature of the parameter space, the problem seems to be a good application arena for PSO, by which the optimal performance of the ML criteria can be fully explored. The design of the optimization algorithm is a combination of the problem-independent PSO kernel and some newly introduced problem-specific features such as search space mapping, particle velocity control, and particle position clipping. This architecture plus properly selected parameters make the PSO algorithm highly flexible and reusable, while being sufficiently specific and effective in the current application. By pairing PSO with the ML criteria, the proposed PSO-ML technique achieves some desired advantages over previous methods: 1) it is less sensitive to initialization, however, insertion of a good initial estimate speeds up the computation; 2) it has better chances to attain the global convergence; 3) it may offer higher quality estimates of the unknown parameters; 4) correlated or even coherent sources can be accurately treated. Via extensive simulation studies, we demonstrate that with the proposed technique, the uncalibrated sensors improve the DOA estimation performance dramatically. PSO-ML produces more accurate estimates of the unknown parameters as compared with other popular methods, which can attain the Cramer Rao bound (CRB) asymptotically; furthermore, it is more efficient in computation.

The paper has been organized as follows. Section II describes the data model. In Section III, we derive the ML algorithm for DOA and array parameter estimation. Section IV presents the principle of PSO, the architecture and implementation of the PSO-ML estimator and the strategies for parameter selection. Simulation results are given in Section V, and Section VI concludes the paper.

Authorized licensed use limited to: STRATHCLYDE UNIVERSITY LIBRARY. Downloaded on July 01,2010 at 09:09:56 UTC from IEEE Xplore. Restrictions apply.

II. DATA MODEL AND PROBLEM FORMULATION

We consider an array of M sensors arranged in an arbitrary geometry and N narrowband far-field signal sources at unknown locations. The complex M-vector of array outputs is modeled by the standard equation

$$\mathbf{y}(t) = \mathbf{A}(\boldsymbol{\theta})\mathbf{s}(t) + \mathbf{n}(t), \qquad t = 1,2,\ldots,L \tag{1}$$

where $\boldsymbol{\theta} = [\theta_1,\ldots,\theta_N]^{\mathrm{T}}$ is the source DOA vector, and the kth column of the complex $M \times N$ matrix $\mathbf{A}(\boldsymbol{\theta})$ is the so-called steering vector $\mathbf{a}(\theta_k)$ for the DOA θ_k. The ith element $a_i(\theta_k)$ models the gain and phase adjustments (with respect to a reference point) of the kth signal at the ith sensor. Furthermore, the complex N-vector $\mathbf{s}(t)$ is composed of the emitter signals, and $\mathbf{n}(t)$ models the additive noise.

The vectors of signals and noise are assumed to be stationary, temporally white, zero-mean complex Gaussian random processes with second-order moments given by

$$\begin{aligned} E\{\mathbf{s}(t)\mathbf{s}^{\mathrm{H}}(s)\} &= \mathbf{P}\delta_{ts} \\ E\{\mathbf{s}(t)\mathbf{s}^{\mathrm{T}}(s)\} &= 0 \\ E\{\mathbf{n}(t)\mathbf{n}^{\mathrm{H}}(s)\} &= \sigma^2\mathbf{I}\delta_{ts} \\ E\{\mathbf{n}(t)\mathbf{n}^{\mathrm{T}}(s)\} &= 0 \end{aligned} \tag{2}$$

where δ_{ts} is the Kronecker delta, $(\cdot)^{\mathrm{H}}$ denotes complex conjugate transpose, $(\cdot)^{\mathrm{T}}$ denotes transpose, $E[\cdot]$ stands for expectation, and $\mathbf{P}$ and $\sigma^2\mathbf{I}$ are the signal and noise covariance matrices, respectively. Assuming that the noise and signals are independent, the data covariance matrix is given by

$$\mathbf{R} = E\{\mathbf{y}(t)\mathbf{y}^{\mathrm{H}}(t)\} = \mathbf{A}\mathbf{P}\mathbf{A}^{\mathrm{H}} + \sigma^2\mathbf{I}. \tag{3}$$

We focus on the case where some of the array sensors are uncalibrated. Without loss of generality, it is assumed that the first K sensors are calibrated, while the last $J = M - K$ sensors are uncalibrated. Furthermore, it is assumed that K is larger than N (known or estimated) as in [9], [17], in order to guarantee the identifiability of unknown parameters. We use the following model for $\mathbf{A}$

$$\mathbf{A} = \begin{bmatrix} \mathbf{A}_1(\boldsymbol{\theta}) \\ \mathbf{A}_2 \end{bmatrix} \tag{4}$$

where $\mathbf{A}_1(\boldsymbol{\theta})$ consists of the first K rows of $\mathbf{A}$ corresponding to the K calibrated sensors, and $\mathbf{A}_2$ consists of the last J rows of $\mathbf{A}$ and associates with the other J uncalibrated sensors. The (i,k)th element $a_i(\theta_k)$ of $\mathbf{A}_2$ has the form

$$a_i(\theta_k) = g_i e^{j\psi_{ik}}, \qquad i = 1,\ldots,J, \quad k = 1,\ldots,N \tag{5}$$

where g_i is the element gain term, and ψ_{ik} is the individual phase term given by

$$\psi_{ik} = 2\pi f_s \tau_i(\theta_k) + \phi_{ik} \tag{6}$$

where f_s is the center frequency, $\tau_i(\theta_k)$ is the relative time delay between reference point and the ith sensor for the kth signal, and ϕ_{ik} is the uncompensated phase error of the kth signal at the ith sensor.

We assume that the uncalibrated sensors have unknown direction independent gain g_i in (5). The assumption is suitable for most practical systems, since the sensor gains do not change much with direction and a typical change is 1 dB [17]. Although this assumption appears to restrict the sensors to be omni-directional, the model can cover the case of sensors with direction-dependent gains as well with little modification. Since the phase values ψ_{ik} are treated as free parameters, the expression in (5) accounts for a relatively broad range of imperfect array problems including arbitrary sensor position errors, phase distortion due to, e.g., the near field effect, and random sensor phase errors.

We define

$$\mathbf{g} = [g_1,\ldots,g_J]^{\mathrm{T}} \tag{7}$$

$$[\boldsymbol{\Psi}]_{ik} = \psi_{ik}, \qquad i = 1,\ldots,J, \quad k = 1,\ldots,N \tag{8}$$

for the unknown sensor gains and phases. The problem addressed herein is the joint estimation of $\boldsymbol{\theta}$, $\mathbf{g}$ and $\boldsymbol{\Psi}$, from a batch of L measurements $\mathbf{y}(1),\ldots,\mathbf{y}(L)$.

III. MAXIMUM LIKELIHOOD SOURCE AND ARRAY PARAMETER ESTIMATION

As a chief systematic approach to most estimation problems, the ML method is known to be asymptotically (with large number of snapshots) unbiased and statistically efficient. This technique requires a probabilistic setup of the problem at hand. Under the assumption of additive Gaussian noise and Gaussian distributed emitter signals, and deterministic unknown gains and phases of uncalibrated sensors, the probability density function of the complete data set is given by

$$f(\mathbf{y}(1),\ldots\mathbf{y}(L) \mid \boldsymbol{\theta},\mathbf{g},\boldsymbol{\Psi},\mathbf{P},\sigma^2) = \prod_{t=1}^{L} \frac{1}{|\pi\mathbf{R}|} e^{-\mathbf{y}^{\mathrm{H}}(t)\mathbf{R}^{-1}\mathbf{y}(t)} \tag{9}$$

where $|\cdot|$ denotes the determinant. By ignoring parameter-independent terms, maximization of (9) is equivalent to minimizing the following normalized negative log-likelihood function

$$I(\boldsymbol{\theta},\mathbf{g},\boldsymbol{\Psi},\mathbf{P},\sigma^2) = \log|\mathbf{R}| + \mathrm{tr}\{\mathbf{R}^{-1}\hat{\mathbf{R}}\} \tag{10}$$

where $\mathrm{tr}\{\cdot\}$ stands for trace, $\log|\cdot|$ denotes the natural logarithm of the determinant, and $\hat{\mathbf{R}}$ is the covariance matrix of the measured data

$$\hat{\mathbf{R}} = \frac{1}{L}\sum_{t=1}^{L} \mathbf{y}(t)\mathbf{y}^{\mathrm{H}}(t). \tag{11}$$

Authorized licensed use limited to: STRATHCLYDE UNIVERSITY LIBRARY. Downloaded on July 01,2010 at 09:09:56 UTC from IEEE Xplore. Restrictions apply.

It assumes that the asymptotic covariance matrix $\mathbf{R}$ is known in (10). However, this is not the case in practice. Besides the parameters of interest, the function (10) also depends on $\mathbf{P}$ and σ^2. To reduce the search dimension, we can solve $\mathbf{P}$ and σ^2 as the functions of $\boldsymbol{\theta}$, $\mathbf{g}$, and $\boldsymbol{\Psi}$, and substitute them back into the likelihood function. Following similar derivations in [28], the ML estimates of σ^2 and $\mathbf{P}$ are given by

$$\hat{\sigma}^2(\boldsymbol{\theta},\mathbf{g},\boldsymbol{\Psi}) = \frac{1}{M-N}\mathrm{tr}\{\mathbf{P}_A^{\perp}\hat{\mathbf{R}}\} \tag{12}$$

$$\hat{\mathbf{P}}(\boldsymbol{\theta},\mathbf{g},\boldsymbol{\Psi}) = \bar{\mathbf{A}}(\hat{\mathbf{R}} - \hat{\sigma}^2\mathbf{I})\bar{\mathbf{A}}^{\mathrm{H}} \tag{13}$$

where $\bar{\mathbf{A}} = (\mathbf{A}^{\mathrm{H}}\mathbf{A})^{-1}\mathbf{A}^{\mathrm{H}}$, $\mathbf{P}_A = \mathbf{A}\bar{\mathbf{A}}$, and $\mathbf{P}_A^{\perp} = \mathbf{I} - \mathbf{P}_A$. For conciseness, the dependence of $\mathbf{A}$ on $\boldsymbol{\theta}$, $\mathbf{g}$, and $\boldsymbol{\Psi}$ has been suppressed. Substituting (12) and (13) into (10), we get (in large samples)

$$I(\boldsymbol{\theta},\mathbf{g},\boldsymbol{\Psi}) = \log|\mathbf{A}\hat{\mathbf{P}}\mathbf{A}^{\mathrm{H}} + \hat{\sigma}^2\mathbf{I}|. \tag{14}$$

The ML estimate of DOAs and sensor gains and phases is computed by minimizing the cost function (14) with respect to the $N + J + NJ$ unknown real parameters. We note that (14) has a similar format as the stochastic ML DOA estimator in [29], however, (14) depends on both source and system parameters. Although the extension is straightforward and not complicated in mathematics, the resulting estimator is effective.

The CRB provides a lower bound on the covariance matrix of any unbiased estimator, and is expected to be a good performance predictor for large samples. Weiss and Friedlander's method [17], or Weiss' method in short, is a well-known technique for joint estimation of DOAs and unknown array parameters with a PCA. To make the study complete and for the convenience of evaluating the proposed technique, Weiss' method and CRB expressions are described briefly as follows [17].

1) *Weiss' Method*: We consider the eigendecomposition of the data covariance matrix (3)

$$\mathbf{R} = \mathbf{A}\mathbf{P}\mathbf{A}^{\mathrm{H}} + \sigma^2\mathbf{I} = \mathbf{U}_s\boldsymbol{\Lambda}_s\mathbf{U}_s^{\mathrm{H}} + \sigma^2\mathbf{U}_n\mathbf{U}_n^{\mathrm{H}} \tag{15}$$

where $\boldsymbol{\Lambda}_s = \mathrm{diag}\{\lambda_1,\ldots,\lambda_N\}$ is a diagonal matrix (when the sources are uncorrelated) containing the N biggest eigenvalues in decreasing order, and the associated eigenvectors are the columns of $\mathbf{U}_s$. $\mathbf{U}_n$ contains the remaining $M-N$ eigenvectors associated with the eigenvalues $\lambda_{N+1} = \cdots = \lambda_M = \sigma^2$. Subtracting $\sigma^2\mathbf{I} = \sigma^2(\mathbf{U}_s\mathbf{U}_s^{\mathrm{H}} + \mathbf{U}_n\mathbf{U}_n^{\mathrm{H}})$ from (15) we get

$$\mathbf{A}\mathbf{P}\mathbf{A}^{\mathrm{H}} = \mathbf{U}_s\boldsymbol{\Gamma}_s\mathbf{U}_s^{\mathrm{H}} \tag{16}$$

where $\boldsymbol{\Gamma}_s = \mathrm{diag}\{\lambda_1 - \sigma^2,\ldots,\lambda_N - \sigma^2\}$. This can be rewritten as

$$\mathbf{A}\mathbf{P}^{1/2} = \mathbf{U}_s\boldsymbol{\Gamma}_s^{1/2}\mathbf{Q} \tag{17}$$

where $\mathbf{Q}$ is an orthonormal matrix. The eigendecomposition of the sample covariance matrix $\hat{\mathbf{R}}$ (11) provides the estimates $\hat{\mathbf{U}}_s$ and $\hat{\boldsymbol{\Gamma}}_n$ of $\mathbf{U}_s$ and $\boldsymbol{\Gamma}_n$, respectively. We can put this together to get the optimization problem

$$\arg\min_{\boldsymbol{\theta},\mathbf{g},\boldsymbol{\Psi}} \|\mathbf{A}\hat{\mathbf{P}}^{1/2} - \hat{\mathbf{U}}_s\hat{\boldsymbol{\Gamma}}_s^{1/2}\mathbf{Q}\|_F^2 \tag{18}$$

whose minimum corresponds to the estimates of DOAs and steering vectors.

2) *The CRB for DOA Estimation*:

$$\mathrm{CRB}_{\boldsymbol{\theta}} = \frac{1}{2L}\{\mathrm{Re}[(\mathbf{P}\mathbf{A}^{\mathrm{H}}\mathbf{R}^{-1}\mathbf{A}\mathbf{P})\odot(\dot{\mathbf{A}}^{\mathrm{H}}\mathbf{R}^{-1}\dot{\mathbf{A}})^{\mathrm{T}} + (\mathbf{P}\mathbf{A}^{\mathrm{H}}\mathbf{R}^{-1}\dot{\mathbf{A}})\odot(\mathbf{P}\mathbf{A}^{\mathrm{H}}\mathbf{R}^{-1}\dot{\mathbf{A}})^{\mathrm{T}}]\}^{-1} \tag{19}$$

where $\odot$ denotes the Hadamard matrix product, $\mathrm{Re}[\cdot]$ denotes the real part, and

$$\dot{\mathbf{A}} = \left[\left.\frac{\partial\mathbf{A}}{\partial\theta}\right|_{\theta=\theta_1},\ldots,\left.\frac{\partial\mathbf{A}}{\partial\theta}\right|_{\theta=\theta_N}\right]. \tag{20}$$

3) *The CRB for Gain Estimation*:

$$\mathrm{CRB}_{\mathbf{g}} = \frac{1}{2L}\{\mathrm{Re}[\mathbf{H}[(\mathbf{C}\mathbf{P}\mathbf{A}^{\mathrm{H}}\mathbf{R}^{-1})\odot(\mathbf{C}\mathbf{P}\mathbf{A}^{\mathrm{H}}\mathbf{R}^{-1})^{\mathrm{T}} + (\mathbf{C}\mathbf{P}\mathbf{A}^{\mathrm{H}}\mathbf{R}^{-1}\mathbf{A}\mathbf{P}\mathbf{C}^{\mathrm{H}})\odot(\mathbf{R}^{-1})^{\mathrm{T}}]\mathbf{H}^{\mathrm{T}}]\}^{-1} \tag{21}$$

where

$$\mathbf{C} = \begin{bmatrix}\mathbf{A}_1(\boldsymbol{\theta})\\ \mathbf{A}_{\Psi}\end{bmatrix},$$

$$[\mathbf{A}_{\Psi}]_{ik} = e^{j[\Psi]_{ik}}, \qquad i = 1,\ldots,J, \quad k = 1,\ldots,N$$

the $J\times M$ matrix

$$[\mathbf{H}]_{ik} = \begin{cases}1 & \text{if} \quad k = K+i\\ 0 & \text{otherwise}\end{cases},$$

$J = M - K$, and K is the number of calibrated sensors.

4) *The CRB for Phase Estimation*:

$$\begin{aligned}\mathrm{CRB}_{\boldsymbol{\Psi}} = \frac{1}{2L}\{\mathrm{Re}[&-[\mathrm{vec}\{\mathbf{H}\mathbf{A}\}\mathrm{vec}^{\mathrm{T}}\{\mathbf{H}\mathbf{A}\}]\\ &\odot[\mathbf{v}_N\otimes(\mathbf{P}\mathbf{A}^{\mathrm{H}}\mathbf{R}^{-1}\mathbf{H}^{\mathrm{T}})^{\mathrm{T}}\otimes\mathbf{v}_J^{\mathrm{T}}]\\ &\odot[\mathbf{v}_N^{\mathrm{T}}\otimes(\mathbf{P}\mathbf{A}^{\mathrm{H}}\mathbf{R}^{-1}\mathbf{H}^{\mathrm{T}})\otimes\mathbf{v}_J]\\ &+[\mathrm{vec}\{\mathbf{H}\mathbf{A}\}\mathrm{vec}^{\mathrm{T}}\{(\mathbf{A}^{\mathrm{H}}\mathbf{H}^{\mathrm{T}})^{\mathrm{T}}\}]\\ &\odot[(\mathbf{v}_N\mathbf{v}_N^{\mathrm{T}})\otimes(\mathbf{H}\mathbf{R}^{-1}\mathbf{H}^{\mathrm{T}})^{\mathrm{T}}]\\ &\odot[(\mathbf{P}\mathbf{A}^{\mathrm{H}}\mathbf{R}^{-1}\mathbf{A}\mathbf{P})\otimes(\mathbf{v}_J\mathbf{v}_J^{\mathrm{T}})]]\}^{-1}\end{aligned} \tag{22}$$

where $\mathrm{vec}\{\cdot\}$ is a concatenation of the columns of the bracketed matrix, $\otimes$ denotes Kronecker product, and $\mathbf{v}_p$ stands for a $p\times 1$ vector of ones.

IV. PARTICLE SWARM OPTIMIZATION FOR MAXIMUM LIKELIHOOD ESTIMATION

PSO is a stochastic optimization paradigm inspired by social behavior of organisms such as bird flocking

Authorized licensed use limited to: STRATHCLYDE UNIVERSITY LIBRARY. Downloaded on July 01,2010 at 09:09:56 UTC from IEEE Xplore. Restrictions apply.

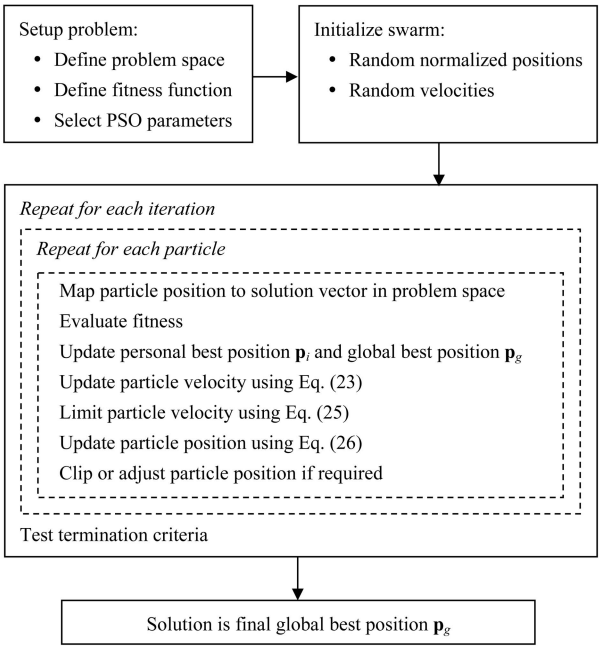

Fig. 1. Flowchart illustrating main steps of PSO-ML estimator.

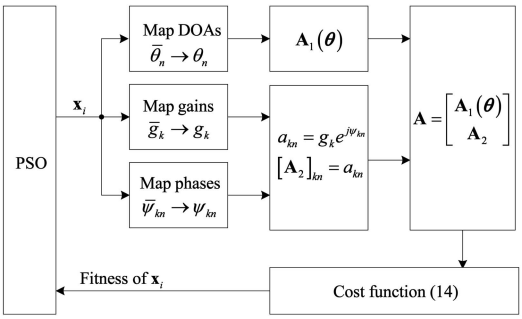

Fig. 2. Flowchart depicting determination of particle fitness.

and fish schooling [21]. As illustrated in Fig. 1, the algorithm starts by initializing a population of particles in the "normalized" search space with random positions $\mathbf{x}$ and velocities $\mathbf{v}$ constrained between zero and one in each dimension. The position vector of the ith particle takes the form $\mathbf{x}_i = [\bar{\theta}_1, \ldots \bar{\theta}_N, \bar{g}_1, \ldots \bar{g}_J, \bar{\psi}_{11}, \ldots, \bar{\psi}_{JN}]$, where $0 < \bar{\theta}_n, \bar{g}_k, \bar{\psi}_{kn} \leq 1$, $n = 1, \ldots, N$, $k = 1, \ldots, J$, $N \geq 1$, and $J \geq 1$. The fitness of each particle is computed based on the flowchart in Fig. 2. At first, the normalized DOA, gain, and phase values are mapped and scaled to the desired ranges; then, the steering vector components corresponding to the calibrated sensors and uncalibrated sensors are determined; and finally the fitness of the particle is evaluated using the cost function (14).

The ith particle's velocity is updated according to (23)

$$\mathbf{v}_i^{k+1} = \omega^k \mathbf{v}_i^k + c_1 \mathbf{r}_1^k \odot (\mathbf{p}_i^k - \mathbf{x}_i^k) + c_2 \mathbf{r}_2^k \odot (\mathbf{p}_g^k - \mathbf{x}_i^k) \tag{23}$$

where $\mathbf{p}_i$ is the best previous position of the ith particle, $\mathbf{p}_g$ is the best position found by any particle in the swarm, $\odot$ denotes element-wise product, $k = 1, 2, \ldots$ indicates the iterations, ω is a parameter called the inertia weight, c_1 and c_2 are positive constants referred to as cognitive and social parameters, respectively, and $\mathbf{r}_1$ and $\mathbf{r}_2$ are independent random vectors. Three components typically contribute to the new velocity. The first part refers to the inertial effect of the movement. The inertial weight ω is considered critical for the convergence behavior of PSO [30]. A larger ω facilitates searching new area and global exploration while a smaller ω tends to facilitate fine exploitation in the current search area. In this study, ω is selected to decrease during the optimization process. Given a maximum value $\omega_{\max}$ and a minimum value $\omega_{\min}$, ω is updated as follows:

$$\omega^k = \begin{cases} \omega_{\max} - \dfrac{\omega_{\max} - \omega_{\min}}{rK}(k-1), & 1 \leq k \leq [rK] \\ \omega_{\min}, & [rK]+1 \leq k \leq K \end{cases} \tag{24}$$

where $[rK]$ is the number of iterations with time decreasing inertial weights, $0 < r < 1$ is a ratio, and K is the maximum iteration number. The second and third components introduce stochastic tendencies to return towards the particle's own best historical position and the group's best historical position. Constants c_1 and c_2 are used to bias the particle's search towards the two locations.

Since there was no actual mechanism for controlling the velocity of a particle, it is necessary to define a maximum velocity to avoid the danger of swarm explosion and divergence [31]. The velocity limit is applied to $\mathbf{v}_i$ along each dimension separately by

$$v_{id} = \begin{cases} V_{\text{MAX}}, & v_{id} > V_{\text{MAX}} \\ -V_{\text{MAX}}, & v_{id} < -V_{\text{MAX}} \end{cases} \tag{25}$$

where $d = 1, \ldots, N + J + NJ$. Like the inertial weight, large values of V_{MAX} encourage global search while small values enhance local search.

The new particle position is calculated using (26),

$$\mathbf{x}_i^{k+1} = \mathbf{x}_i^k + \mathbf{v}_i^{k+1}. \tag{26}$$

If any dimension of the new position vector is less than zero or greater than one, it is clipped to stay within this range. It should be noted that, at any time of the optimization process, two components representing DOAs in a position vector are not allowed to be equal. The final global best position $\mathbf{p}_g$ is taken as the ML estimates of source and array parameters. PSO is robust to control parameters, and some works demonstrate that the performance is not significantly affected by changing the swarm size P [32]. More detailed information on the PSO algorithm and parameter selection strategies is provided in

Authorized licensed use limited to: STRATHCLYDE UNIVERSITY LIBRARY. Downloaded on July 01,2010 at 09:09:56 UTC from IEEE Xplore. Restrictions apply.

TABLE I
Selected PSO Parameters

Parameter	c_1	c_2	P	V_{MAX}	ω_{max}	ω_{min}	r
Value	2.0	2.0	30	0.5	0.9	0.4	0.5

[21], and the analysis of convergence and stability is presented in [31].

V. SIMULATION RESULTS

This section provides three examples to illustrate the superior performance of the PSO-ML algorithm, with a comparison against Weiss's method [17], which is chosen because it has the same function and is based on a similar data model. The root-mean-squared error (RMSE) of the estimates of source DOAs, phases of steering vectors, and sensor gains obtained using the two methods are evaluated and compared, and against the CRB. The RMSE of $\boldsymbol{\theta}$, $\mathbf{g}$, and $\boldsymbol{\Psi}$ is calculated in an average manner as

$$\text{RMSE} = \sqrt{\frac{1}{nN_{\text{runs}}}\sum_{l=1}^{N_{\text{runs}}}\sum_{i=1}^{n}[\hat{\alpha}_i(l)-\alpha_i]^2} \qquad (27)$$

where n equals to N, J and NJ, respectively, N_{runs} is the number of runs, $\hat{\alpha}_i(l)$ is the estimate of the ith parameter achieved in the lth run, and α_i is the true value of the parameter. We have performed 300 Monte Carlo experiments for each point of the plot. The signal-to-noise ratio (SNR) is defined at a single sensor.

The PSO parameters chosen for all the experiments are summarized in Table I. These values are determined based on empirical practice [21, 31–34] and adequate test runs, although a better optimization performance could be potentially achieved by fine-tuning the values. The PSO algorithm starts with a random initialization, and is terminated if the maximum iteration number is reached or the global best particle position is not updated in 50 successive iterations. Weiss' method is initialized with the ML DOA estimates obtained using the calibrated portion of the array. It has been observed that good initialization is crucial for Weiss' method to achieve meaningful results, which is a common drawback for Newton-type procedures.

A. Example 1

In the first example, we consider a uniform linear array (ULA) of 8 elements with sensor separation of half a wavelength. The first 6 sensors are calibrated while the others are not. All the sensors are omnidirectional with unit gain. Two uncorrelated equal-power emitters are present at DOAs 80° and 83° relative to the array end-fire. The number of snapshots is 100, and the SNR is varied. Fig. 3 depicts the DOA estimation RMSE obtained using PSO-ML and Weiss' method with the PCA. For comparison, the dotted line shows the RMSE when only 6 calibrated elements are considered and the uncalibrated elements are ignored, while the dashdot line illustrates the performance of a perfectly calibrated ULA of 8 sensors. It is clear from the figure that uncalibrated sensors may improve the DOA estimation performance. PSO-ML outperforms Weiss' method in the whole SNR range by demonstrating less RMSE, especially when the SNR is low. It is interesting to note that when the SNR is lower than 10 dB, the PCA with PSO-ML performs as well as a perfectly calibrated eight-sensor ULA. It seems that the contribution of the uncalibrated sensors becomes more significant when the array is forced to operate in less favorable conditions: low SNR and closely spaced sources.

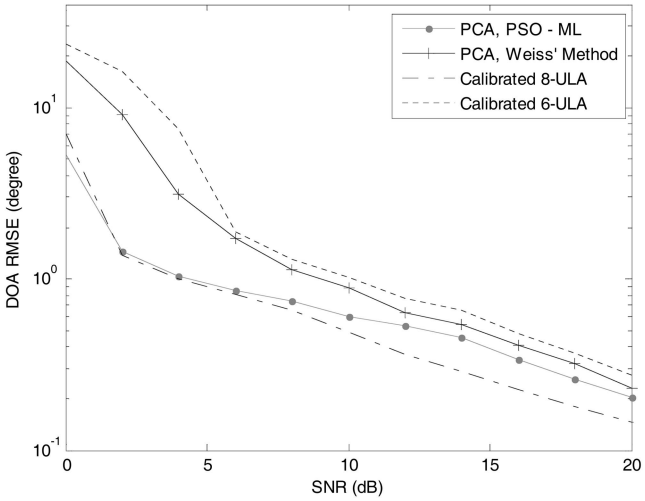

Fig. 3. DOA estimation RMSE versus SNR. Two uncorrelated sources impinge on eight-element ULA at 80° and 83°. Number of snapshots is 100.

Fig. 4 shows the RMSE for estimating the phases of the steering vectors obtained using PSO-ML and Weiss' method, and compares them with the CRB. Fig. 5 illustrates the RMSE of sensor gain estimation for the same methods and the corresponding CRB. As can be seen from Fig. 4 and Fig. 5, for both phase and gain estimation, PSO-ML produces more accurate estimates than Weiss' method, with the RMSE approaching and asymptotically attaining the CRB. It seems that the accuracy of PSO-ML for phase and gain estimation is not sensitive to the SNR. Although Weiss' method produces asymptotically efficient estimates, it demonstrates a strong threshold effect in the phase curve when the SNR is lower than 16 dB.

Fig. 6 depicts the fitness progress curves of PSO-ML obtained with random initialization and preestimated DOA based initialization, respectively. The curves, which are plots of the fitness values of the global best particles versus the iteration

Authorized licensed use limited to: STRATHCLYDE UNIVERSITY LIBRARY. Downloaded on July 01,2010 at 09:09:56 UTC from IEEE Xplore. Restrictions apply.

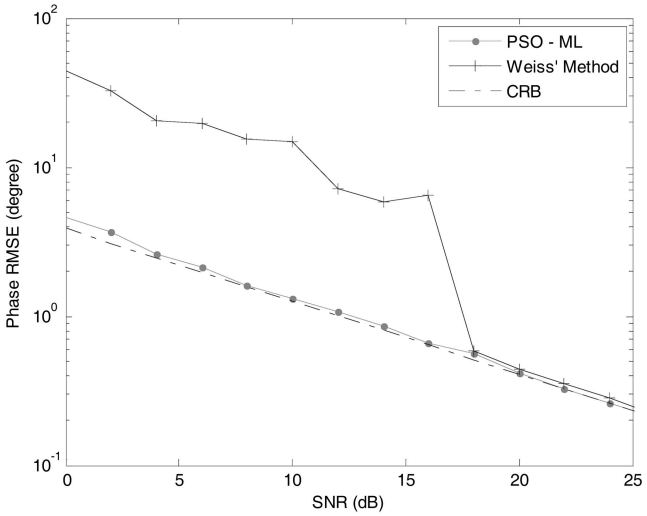

Fig. 4. RMSE of steering vector phase estimation versus SNR. Dashdot line represents theoretic CRB. Two uncorrelated sources impinge on eight-element ULA at 80° and 83°. Number of snapshots is 100.

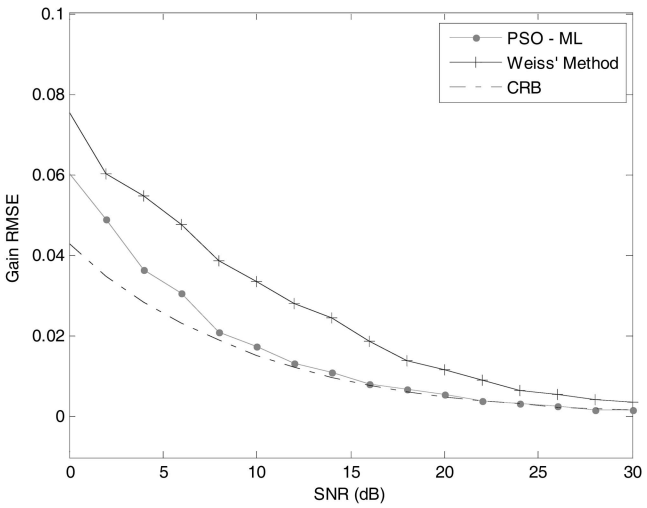

Fig. 5. RMSE of sensor gain estimation versus SNR. Dashdot line represents theoretic CRB. Two uncorrelated sources impinge on eight-element ULA at 80° and 83°. Number of snapshots is 100.

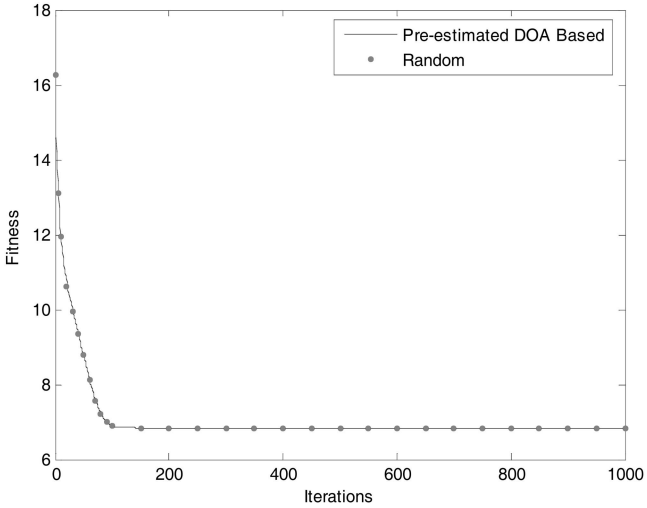

Fig. 6. Fitness progress curves of PSO-ML obtained with random initialization and preestimated DOA-based initialization. Dimension of problem space is 8; number of DOA estimates is 2.

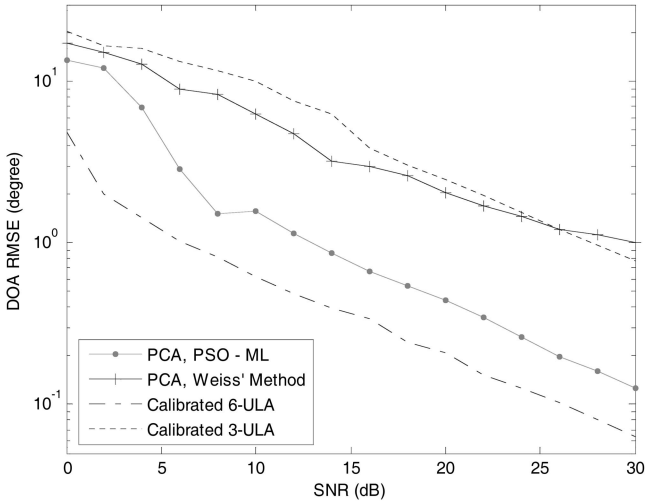

Fig. 7. DOA estimation RMSE versus SNR. Two correlated sources impinge on six-element ULA at 90° and 96°, $\kappa = 0.8$. Number of snapshots is 60.

number, are obtained over an average of 300 runs. The initial DOA estimates are calculated using the ML algorithm with the calibrated portion of the array. As can be seen from Fig. 6, PSO achieves fast convergence with the selected parameters, and the smooth dropping curve means that the global best particle is continuously updated in each iteration. Furthermore, PSO is not sensitive to initial particle positions, and two initialization methods make almost the same convergence progress. In this example, the PSO with random initialization achieves convergence with an average iteration number of about 200, and PSO-ML is approximately 15 times more efficient in computation than Weiss' method.

B. Example 2

In the second example, the proposed technique is examined in more unfavorable conditions. We assume that two equal-power, correlated signals with the correlation factor $\kappa = 0.8$ impinge on a ULA of 6 unit gain elements with half-wavelength spacing from 90° and 96° relative to the end-fire. The first 3 sensors are calibrated while the others are not. The number of snapshots is 60. Fig. 7 depicts the DOA estimation RMSE obtained using PSO-ML and Weiss' method with the PCA. The dotted line shows the RMSE when only 3 calibrated elements are considered, while the dashdot line illustrates the performance of a perfectly calibrated ULA of 6 sensors. The PSO-ML algorithm may treat scenarios involving correlated signals (in fact, even coherent sources) without difficulties. Compared with the dotted line obtained using the

Authorized licensed use limited to: STRATHCLYDE UNIVERSITY LIBRARY. Downloaded on July 01,2010 at 09:09:56 UTC from IEEE Xplore. Restrictions apply.

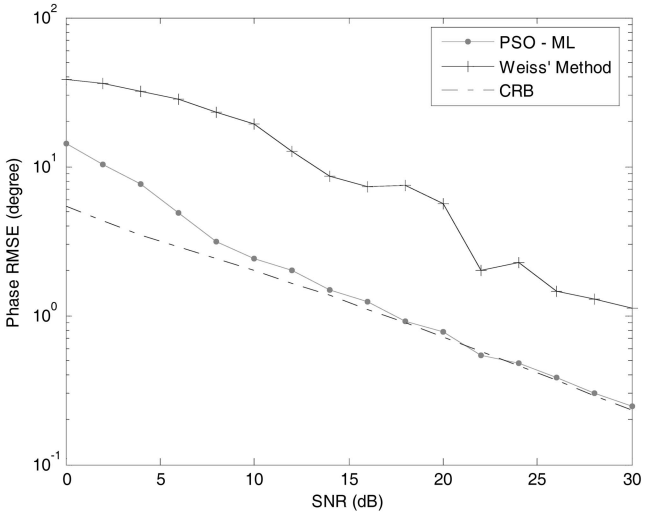

Fig. 8. RMSE of steering vector phase estimation versus SNR. Dashdot line represents theoretic CRB. Two correlated sources impinge on six-element ULA at 90° and 96°, $\kappa = 0.8$. Number of snapshots is 60.

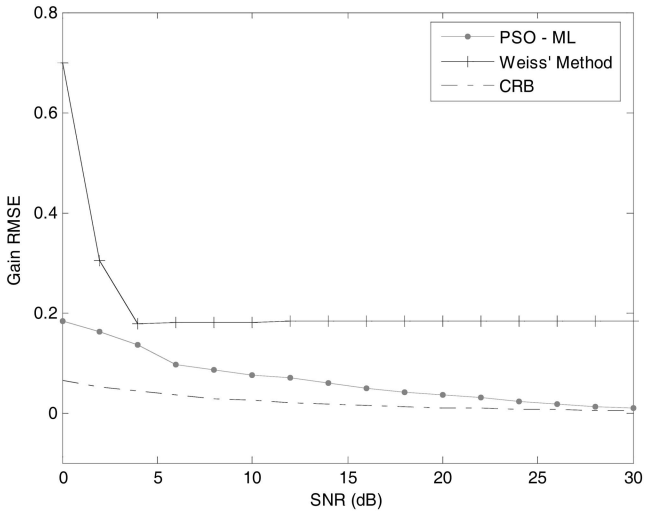

Fig. 9. RMSE of sensor gain estimation versus SNR. Dashdot line represents theoretic CRB. Two correlated sources impinge on six-element ULA at 90° and 96°, $\kappa = 0.8$. Number of snapshots is 60.

three-element ULA, the uncalibrated sensors with PSO-ML improve the performance significantly, and yield good DOA estimates. However, Weiss' method encounters problems in this scenario, and the estimates are not accurate even in high SNR.

Fig. 8 shows the RMSE for estimating the phases of the steering vectors obtained using PSO-ML and Weiss' method, and compares them with the CRB. Fig. 9 illustrates the RMSE of sensor gain estimation for the same methods and the corresponding CRB. It is clear from Fig. 8 and Fig. 9 that for both phase and gain estimation, PSO-ML produces accurate estimates with the RMSE approaching and asymptotically attaining the CRB. The RMSE curves don't demonstrate strong threshold effect. On the other hand, due to the existence of correlated signals, the performance of Weiss' method is unsatisfactory, the RMSE curves of both phase and gain estimation could not approach and asymptotically attain the CRB.

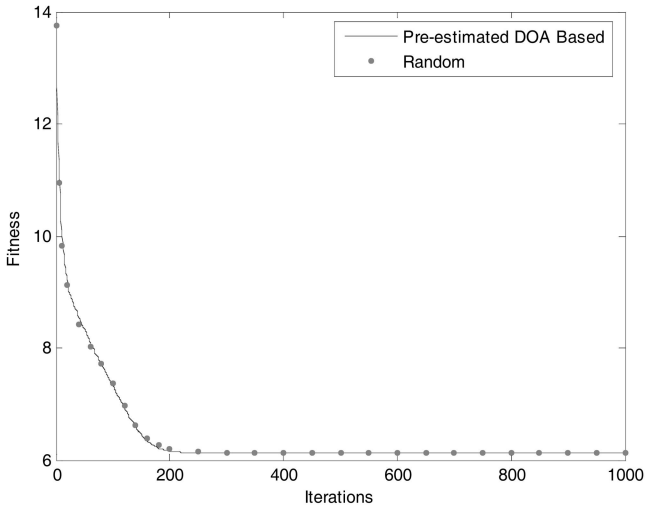

Fig. 10. Fitness progress curves of PSO-ML obtained with random initialization and preestimated DOA-based initialization. Dimension of problem space is 11; number of DOA estimates is 2.

Fig. 10 shows the fitness progress curves of PSO-ML starting from random initialization and preestimated DOA based initialization, respectively. Again, PSO attains fast and smooth convergence, regardless of the initialization methods. As compared with the curves in Fig. 6, the fitness progress drops more gently, because the problem space has a higher dimension and maybe is more complex in nature. In this example, PSO-ML is approximately 5 times more efficient in computation than Weiss' method, and the average number of iterations to attain convergence is about 350.

C. Example 3

In the third example, a different scenario is studied and the performance of PSO-ML is examined as a function of snapshots L. We consider a half-radius uniform circular array (UCA) of 8 elements, 6 calibrated and 2 uncalibrated. The sources are 2 correlated signals with unequal power present at 60° and 70°, $\kappa = 0.9$, $p_1 = 0.8p_2$, where p_1 and p_2 are the power of the two signals.

Fig. 11 depicts the DOA estimation RMSE obtained using PSO-ML and Weiss' method with the PCA, when SNR is 15 dB and 20 dB, respectively. The RMSE corresponding to the perfectly calibrated eight-element UCA is also illustrated for comparison. Fig. 12 and Fig. 13 demonstrate the RMSE of sensor phase and gain estimation for the same methods and SNRs, and compare them with the corresponding CRB. It is worth noting that for correlated signals with unequal power, PCA with PSO-ML produces

Authorized licensed use limited to: STRATHCLYDE UNIVERSITY LIBRARY. Downloaded on July 01,2010 at 09:09:56 UTC from IEEE Xplore. Restrictions apply.

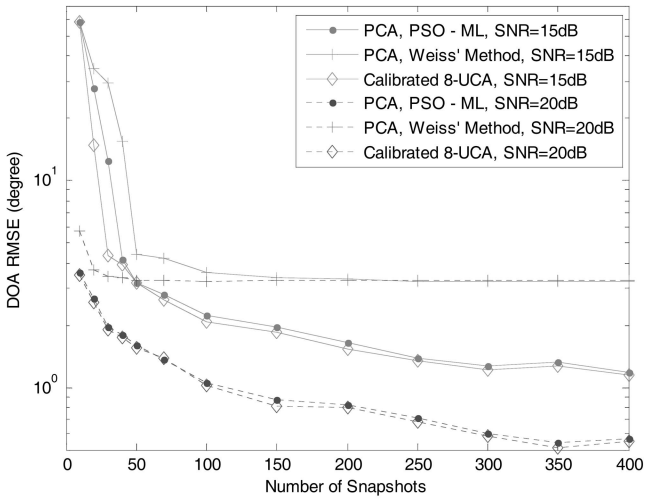

Fig. 11. DOA estimation RMSE versus number of snapshots. Two correlated sources with unequal power impinge on eight-element UCA at 60° and 70°, $\kappa = 0.9$, $p_1 = 0.8p_2$.

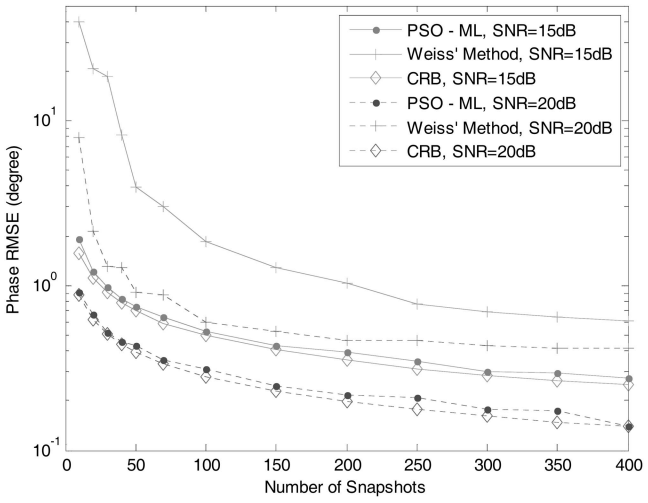

Fig. 12. RMSE of steering vector phase estimation versus number of snapshots. Two correlated sources with unequal power impinge on eight-element UCA at 60° and 70°, $\kappa = 0.9$, $p_1 = 0.8p_2$.

DOA estimates almost as accurate as the calibrated eight-element UCA for various sample sizes and the two selected SNRs, probably because the uncalibrated sensors don't reduce the array aperture significantly; the threshold effect is observed only when $L < 40$ and SNR = 15 dB; PSO-ML yields excellent gain and phase estimates with RMSE approaching the CRB; and PSO-ML significantly outperforms Weiss' method, which is obsessed by the correlated signals. The benefits and advantages of PSO-ML demonstrated in this example are similar and comparable with SNR-varying scenarios in the first two experiments. When L is very small, the covariance matrix $\hat{\mathbf{R}}$ cannot be estimated accurately, which degrades the DOA and gain estimation of PSO-ML, especially when SNR is low; however, it seems that phase estimation is relatively robust.

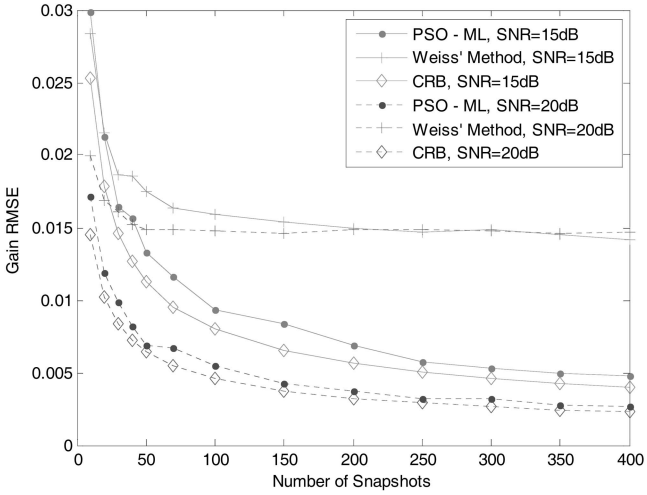

Fig. 13. RMSE of sensor gain estimation versus number of snapshots. Two correlated sources with unequal power impinge on eight-element UCA at 60° and 70°, $\kappa = 0.9$, $p_1 = 0.8p_2$.

For comparison, GA [5] is also applied to the ML problem in the above examples, and it is shown that PSO-ML is roughly 10–15 times more efficient than GA-ML. In the simulations, the number of sources N is assumed to be known. However, this is often not the practical situation, and N must be estimated with the calibrated portion of the array. In general, N can be measured accurately with Akaike's information criterion (AIC) and minimum description length (MDL) techniques [35] except for unfavorable scenarios. If we want to enhance the performance of PSO-ML in the threshold region for low SNRs and short snapshots, a more accurate detection algorithm that can estimate N in hard conditions must be selected. The interested reader may refer to [35], [36] and the references therein.

The superior performance of PSO-ML over Weiss' method observed in numerical examples can be explained by the fact that PSO-ML is based on the statistically optimal ML criteria, while Weiss' method is derived from a MUSIC-like spectral decomposition of the sample covariance matrix, but MUSIC is known to be a suboptimal estimator more suitable for favorable conditions involving high SNR, large sample size, and uncorrelated sources. A common drawback with ML-based techniques is that they are computation extensive and tend to suffer local convergence due to the underlying high-dimensional multimodal problem space, thus a fast and robust global optimization tool is critical.

VI. CONCLUSIONS

This paper addresses the problem of source DOA estimation using a PCA. An interesting but challenging category of solutions to this problem is to estimate the source directions in addition to the estimation of unknown array parameters such

Authorized licensed use limited to: STRATHCLYDE UNIVERSITY LIBRARY. Downloaded on July 01,2010 at 09:09:56 UTC from IEEE Xplore. Restrictions apply.

as sensor gains and phases, as a way of performing array self-calibration. An algorithm based on the ML methodology is derived, where the cost function is an extension of the ML criteria that were originally developed for angle estimation with a perfectly calibrated array. A PSO algorithm is used to explore the high-dimensional complicated problem space and find the global minimum of the cost function. The design of the PSO is a combination of the problem-independent kernel and some newly introduced problem-specific features such as search space mapping, particle velocity control, and particle position clipping. This architecture plus properly selected parameters make the PSO algorithm highly flexible and reusable for other applications, while being sufficiently specific and effective in the current problem. As a result, PSO achieves fast and robust global convergence, and careful initialization is not necessary. Simulation results demonstrate that with the proposed technique, the uncalibrated sensors improve the DOA estimation performance dramatically. PSO-ML produces more accurate estimates of the unknown parameters in a cheaper way as compared with another popular method, with the RMSE approaching and asymptotically attaining the CRB; furthermore, it works well with correlated or even coherent sources.

REFERENCES

[1] Weiss, A. J., and Friedlander, B.
Comparison of signal estimation using calibrated and uncalibrated arrays.
IEEE Transactions on Aerospace and Electronic Systems, **33** (Jan. 1997), 241–249.

[2] Schmidt, R. O.
Multiple emitter location and signal parameter estimation.
IEEE Transactions on Antennas and Propagation, **34** (Mar. 1986), 276–280.

[3] Roy, R., and Kailath, T.
ESPRIT—Estimation of signal parameters via rotational invariance techniques.
IEEE Transactions on Acoustics, Speech and Signal Processing, **37** (July 1989), 984–995.

[4] Viberg, M., Ottersten, B., and Kailath, T.
Detection and estimation in sensor arrays using weighted subspace fitting.
IEEE Transactions on Signal Processing, **39** (Nov. 1991), 2436–2449.

[5] Li, M. H., and Lu, Y. L.
Accurate direction-of-arrival estimation of multiple sources using a genetic approach.
Wireless Communications and Mobile Computing, **5** (May 2005), 343–353.

[6] Li, M. H., and Lu, Y. L.
Dimension reduction for array processing with robust interference cancellation.
IEEE Transactions on Aerospace and Electronic Systems, **42** (Jan. 2006), 103–112.

[7] Yuen, N., and Friedlander, B.
Asymptotic performance analysis of blind signal copy using fourth-order cumulants.
International Journal of Adaptive Control and Signal Processing, **10** (May 1996), 239–265.

[8] See, C. M. S., and Gershamn, A. B.
Direction-of-arrival estimation in partly calibrated subarray-based sensor arrays.
IEEE Transactions on Signal Processing, **52** (Feb. 2004), 329–338.

[9] Stoica, P., Viberg, M., Wong, K. M., and Wu, Q.
Maximum-likelihood bearing estimation with partly calibrated arrays in spatially correlated noise fields.
IEEE Transactions on Signal Processing, **44** (Apr. 1996), 888–899.

[10] Fuhrman, D. R.
Estimation of sensor gain and phase.
IEEE Transactions on Signal Processing, **42** (Jan. 1994), 77–87.

[11] Soon, V. C., Tong, L., Huang, Y. F., and Liu, R.
A subspace method for estimating sensor gains and phases.
IEEE Transactions on Signal Processing, **42** (Apr. 1994), 973–976.

[12] Cheng, Q., Yua, Y., and Stoica, P.
Asymptotic performance of optimal gain-and-phase estimators of sensor arrays.
IEEE Transactions on Signal Processing, **48** (Dec. 2000), 3587–3590.

[13] Vezzosi, G.
Estimation of phase angles from the cross-spectral matrix.
IEEE Transactions on Acoustics, Speech and Signal Processing, **ASSP-34** (June 1986), 405–422.

[14] Wheeler, D. A., and Atkins, P. R.
Estimation of source bearings at a randomly deformed array by signal space transformations.
In *Proceedings of the International Conference on Acoustics, Speech and Signal Processing* (ICASSP), Toronto, Canada, May 1991, 3345–3348.

[15] Li, M. H., and Lu, Y. L.
Maximum likelihood processing for arrays with partially unknown sensor gains and phases.
In *Proceedings of the 7th International Conference on Intelligent Transportation Systems Telecommunications* (ITST'07), Sophia Antipolis, France, June 2007, 185–190.

[16] Tseng, C. Y., Feldman, D. D., and Griffiths, L. J.
Steering vector estimation in uncalibrated arrays.
IEEE Transactions on Signal Processing, **43** (June 1995), 1397–1412.

[17] Weiss, A. J., and Friedlander, B.
DOA and steering vector estimation using a partially calibrated array.
IEEE Transaction on Aerospace and Electronic Systems, **32** (July 1996), 1047–1057.

[18] Li, M. H., and Lu, Y. L.
Improving the performance of GA-ML DOA estimator with a resampling scheme.
Signal Processing, **84** (Oct. 2004), 1813–1822.

[19] Li, M. H., and Lu, Y. L.
Genetic algorithm based maximum likelihood DOA estimation.
In *Proceedings of Radar Conference 2002*, Edinburgh, UK, Oct. 2002, 502–506.

[20] Eberhart, R. C., and Kennedy, J.
A new optimizer using particle swarm theory.
In *Proceedings of the 6th International Symposium on Micro Machine and Human Science* (MHS'95), Nagoya, Japan, Oct. 1995, 39–43.

[21] Li, M. H., and Lu, Y. L.
Maximum likelihood DOA estimation in unknown colored noise field.
IEEE Transaction on Aerospace and Electronic Systems, **44** (July 2008), 1079–1090.

Authorized licensed use limited to: STRATHCLYDE UNIVERSITY LIBRARY. Downloaded on July 01,2010 at 09:09:56 UTC from IEEE Xplore. Restrictions apply.

[22] Boeringer, D. W., and Werner, D. H.
Particle swarm optimization versus genetic algorithms for phased array synthesis.
IEEE Transactions on Antennas and Propagation, **52** (Mar. 2004), 771–779.

[23] Robinson, J., and Rahmat-Samii, Y.
Particle swarm optimization in electromagnetics.
IEEE Transactions on Antennas and Propagation, **52** (Feb. 2004), 397–407.

[24] Gao, Y., and Xie, S.
A blind source separation algorithm using particle swarm optimization.
In *Proceedings of the IEEE 6th Circuits and Systems Symposium on Emerging Technologies: Frontier of Mobile and Wireless Communication*, Shanghai, China, May 2004, 297–300.

[25] Messerschmidt, L., and Engelbrecht, A. P.
Learning to play games using a PSO-based competitive learning approach.
IEEE Transactions on Evolutionary Computation, **8** (June 2004), 280–288.

[26] Abido, M. A.
Optimal power flow using particle swarm optimization.
International Journal of Electrical Power and Energy Systems, **24** (July 2002), 563–571.

[27] Saldam, A., Ahmad, I., and Al-Madani, S.
Particle swarm optimization for task assignment problem.
Microprocessors and Microsystems, **26** (Aug. 2002), 363–371.

[28] Jaffer, A. G.
Maximum likelihood direction finding of stochastic sources: A separable solution.
In *Proceedings of the International Conference on Acoustics, Speech, and Signal Processing* (ICASSP), New York, NY, Apr. 1988, 2893–2896.

[29] Stoica, P., and Nehorai, A.
MUSIC, maximum likelihood, and Cramer-Rao bounds.
IEEE Transactions on Acoustics, Speech and Signal Processing, **37** (May 1989), 720–741.

[30] Parsopoulos, K. E., and Vrahatis, M. N.
Recent approaches to global optimization problems through particle swarm optimization.
Natural Computing, **1** (2002), 235–306.

[31] Clerc, M., and Kennedy, J.
The particle swarm—Explosion, stability, and convergence in a multidimensional complex space.
IEEE Transactions on Evolutionary Computation, **6** (Feb. 2002), 58–73.

[32] Eberhart, R. C., and Shi, Y.
Comparing inertia weights and constriction factors in particle swarm optimization.
In *Proceedings of the Congress on Evolutionary Computation*, vol. 1, Piscataway, NJ, July 2000, 84–88.

[33] Shi, Y., and Eberhart, R. C.
Parameter selection in particle swarm optimization.
In *Proceedings of the 7th International Conference on Evolutionary Programming*, San Diego, CA, Mar. 1998, 591–600.

[34] Shi, Y., and Eberhart, R. D.
A modified particle swarm optimizer.
In *Proceedings of the IEEE World Congress on Computational Intelligence*, Anchorage, AK, May 1998, 69–73.

[35] Godara, L. C.
Application of antenna arrays to mobile communications. Part II: Beam-forming and direction-of-arrival considerations.
Proceedings of the IEEE, **85** (Aug. 1997), 1195–1258.

[36] Li, M. H., Lu, Y. L., Chen, I-M., and Chen, H-H.
High resolution direction-of-arrival estimation and location determination in wireless networks.
International Journal of Computer Research, **16**, 4 (Dec. 2008), 341–370.

Authorized licensed use limited to: STRATHCLYDE UNIVERSITY LIBRARY. Downloaded on July 01,2010 at 09:09:56 UTC from IEEE Xplore. Restrictions apply.

Minghui Li (S'02—M'08) received his B.Sc. and M.Eng. degrees from Xidian University, Xi'an, China, in 1994 and 1999, respectively, and his Ph.D. degree from Nanyang Technological University (NTU), Singapore, in 2004, all in electrical engineering.

From 1994 to 1996, he was an assistant lecturer with the School of Electronic Engineering at Xidian University. From 1999 to 2000, he worked as a research engineer at Siemens Ltd., China. From 2003 to 2008, he was first with the School of Electrical and Electronic Engineering and then the Intelligent Systems Center at NTU as a research fellow. He joined the Department of Electronic & Electrical Engineering, University of Strathclyde, UK as a lecturer in September 2008. His research interests include array design and processing, direction-of-arrival estimation, adaptive and arbitrary beamforming, spatial-temporal processing and coding, smart antennas, OFDM, MIMO, evolutionary computation, wireless sensor networks, and coded ultrasound, with application to radar, sonar, medical diagnosis, nondestructive evaluation, and wireless communications.

Yilong Lu (S'90—M'92) was born in Chengdu, China. He received the B.Eng. degree from Harbin Institute of Technology, China, in 1982, the M.Eng. degree from Tsinghua University, China, in 1984, and the Ph.D. degree in 1991 from University College of London, UK, in 1991, all in electronic engineering.

From 1984 to 1988, he was a faculty member with the Department of Electromagnetic Fields Engineering, University of Electronic Science and Technology of China, Chengdu, China. In 1991, he joined the School of Electrical and Electronic Engineering, Nanyang Technological University, Singapore, where he is currently a professor in the Communication Engineering Division. He was a visiting academic at the University of California–Los Angeles (UCLA) from October 1998 to June 1999. His research interests include antennas, array signal processing, radar systems, computational electromagnetics, and evolutionary computation for engineering optimization.

Authorized licensed use limited to: STRATHCLYDE UNIVERSITY LIBRARY. Downloaded on July 01,2010 at 09:09:56 UTC from IEEE Xplore. Restrictions apply.